eigenvalues for κ_0 and κ_{n+1}, as compared with four for all other κ_i.

The two values κ_{0p} and $-\kappa_{0p}^*$ forming a complex wavepair were already shown[1] to represent a forward and a backward wave, respectively. It should be noted that, for lossless media (ϵ_i and μ_i real), eqn. 9 represents a necessary and sufficient condition for the existence of such a wavepair. If small losses are introduced, one expects from analytic considerations that a wavepair would still be present so that, if κ_{0p} is an eigenvalue, then $\kappa_{0p}' = -\kappa_{0p}^* + \Delta\kappa$ is also an eigenvalue with $|\Delta\kappa/\kappa_{0p}| \ll 1$.

Although the above results were derived for stratified isotropic configurations, the presence of complex wavepairs occurs also in more general cases which include gyrotropic media, cylindrical geometrics, etc. The extension of the results to these more general cases is presently being carried out.

T. TAMIR

3rd April 1967

Department of Electrophysics
Polytechnic Institute of Brooklyn
333 Jay Street, Brooklyn, N Y 11201, USA

References

1 TAMIR, T., and OLINER, A. A.: 'Guided complex waves. Part 1—Fields at an interface', *Proc. IEE*, 1963, **110**, (1), p. 310–324
2 LAXPATI, S. R., and MITTRA, R.: 'Energy considerations in open and closed waveguides', *IEEE Trans.*, 1965, **AP–13**, p. 883
3 CHORNEY, D., BERS, A., and PENFIELD, P.: 'Further generalizations of waveguide theorems', *ibid.*, 1967, **MTT–15**, p. 58

INTEGRATED DIRECT-COUPLED GYRATOR*

An integrated gyrator is described. The device uses 1 diode, 12 resistors and 9 transistors, two of which are lateral *p–n–p*. Experimental results on gyration resistance, input impedance and resonant-circuit *Q* factor show excellent agreement with theory.

Integrated circuits present one of the most attractive approaches for the realisation of low-cost, high-performance gyrators of small enough size that they can be treated as individual components. Like any other circuit, the integrated gyrator must be designed with components producible by integrated-circuit processes. This restriction does not prevent a high-performance circuit from being integrated if the circuit is designed to fully utilise the many inherent advantages offered by integrated circuits. Besides small size, the chief advantages include good component matching, good thermal tracking of all components and a liberal availability of active devices.

To show the feasibility of fully integrating a gyrator, a simple direct-coupled gyrator circuit was designed and integrated using a diffusion process comparable to that used in the mass production of today's commercial integrated circuits. The $0{\cdot}5 \times 10^{-3}$in masking tolerance of the circuit is much looser than that of the present industry standard; therefore, producibility of the circuit is unquestionable.

Numerous transistorised gyrator circuits proposed previously, though generally of high performance, contain one or more of the following characteristics, which make them difficult to be fully integrated inexpensively using present-day integrated-circuit technology: (*a*) m.o.s., *p–n–p* and *n–p–n* transistors in the circuit,[1] (*b*) coupling capacitors or high-quality *p–n–p* and *n–p–n* transistors, or both[2,3,4,5], (*c*) negative resistors or n.i.c.s[6,7,8,9,10], (*d*) high operating supply voltages and power dissipation[11] and (*e*) high complexity.[12,13,14,15]

* Preparation of the manuscript was supportedi n part by the US Air Force Office of Scientific Research under Contract F44620-67-C-0001 and by the US Office of Naval Research Contract Nonr-225 (83)

The circuit used represents a slight modification of that of Rao[16] and is shown in Fig. 1; component designation is as in Reference 16. It contains 12 low-value resistors, 1 diode, 7 *n–p–n* transistors and 2 low-current lateral *p–n–p* transistors on a $0{\cdot}065 \times 0{\cdot}087\text{in}^2$ die (undoubtedly, very much smaller

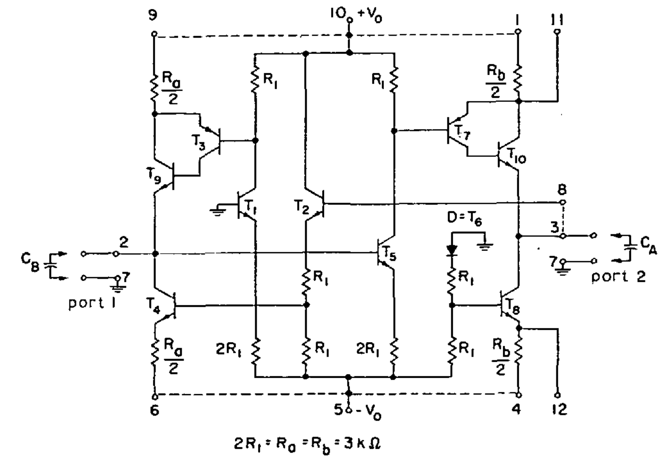

Fig. 1 *Scheme of integrated gyrator*

gyrators can be integrated, but no attempt was made to minimise the die dimensions, as the Stanford step and repeat equipment is only capable of making a fixed size). To allow for further experimentation, such as time variation, there are 12 access points on the chip, as shown in Fig. 1. The dashed lines are (externally) connected for normal operation, but, for example, variable resistors can be placed between points 10–11 and 5–12 if lines 1–10 and 4–5 are opened; of course, all dashed leads could have been directly integrated. The circuit consists of two crosscoupled voltage-controlled current sources, one of which has its output current in phase with the input; the other has its output 180° out of phase with its input voltage. The high output impedance of the current source is normally achieved by a *p–n–p* and an *n–p–n* transistor connected in a push–pull arrangement. Since high-quality floating *p–n–p* transistors are difficult to make in an integrated circuit without using additional diffusion steps, a lateral *p–n–p* transistor[17] was compounded with an *n–p–n* transistor to replace the *p–n–p* transistor. This occurs at transistor pairs T_3–T_9 and T_7–T_{10}; a buried layer is used to reduce the current drained through the resultant (parasitic) substrate *p–n–p* transistor by decreasing carrier lifetime in its base.

The fabrication of the lateral *p–n–p* transistors does not require additional processing; they are made simultaneously with the *n–p–n* transistors. The *p–n–p* basewidths, which have direct effect on their h_{FE}, are easily maintained to within $\pm 20\%$ of the nominal values. The lateral *p–n–p* transistors have h_{FE} approximately equal to unity when operating at collector currents below 500μA, while the *n–p–n* transistors have an h_{FE} of approximately 80. When compounded with an *n–p–n* transistor, the resulting *p–n–p* transistor has an equivalent h_{FE} of

$$h_{FE\,equiv} = h_{FE\,lat\,pnp}(1 + h_{FE\,npn})$$

It is seen that when the h_{FE} of the lateral *p–n–p* is close to unity, the h_{FE} of the equivalent *p–n–p* is very close to the h_{FE} of the *n–p–n* transistor. Consequently the T_3–T_9 and T_7–T_{10} combinations are, respectively, matched with T_4 and T_8 to obtain desirable symmetrical current sources. Other component matchings were achieved by carefully positioning and dimensioning the critical components.

The diffusion process parameters are as follows: substrate resistivity = $1{\cdot}5\Omega$cm, buried layer sheet resistivity = 20Ω, epitaxial resistivity = $0{\cdot}5\Omega$cm, epitaxial thickness = $6{\cdot}2\mu$m, base sheet resistivity = 125Ω, base diffusion depth = $1{\cdot}5\mu$m, emitter sheet resistivity = 3Ω, emitter diffusion depth = 1μm. The design is such that normally the gyration resistance R_G is given by $R_G = R_a = R_b = 3\text{k}\Omega$; for matching purposes, all resistors in the layout are identical and of nominal size $1{\cdot}5\text{k}\Omega$.

The circuit is well compensated for temperature and supply-voltage variations. Measurements showed that R_G remained essentially constant for supply voltages V_0 varying from 4V to 8V. Without using external components, the design target value for R_G is 3kΩ ±20%. As the measured d.c. characteristics of Table 1 show, the R_G obtained were well within expectation. Table 1 also shows that R_G increased by 5·5% when the temperature was raised from 25°C to 100°C. This is entirely due to the positive temperature coefficients of R_a and R_b. The layout of the circuit is such that R_a and R_b may be completely bypassed, and more stable resistors may be connected externally to the gyrator to obtain higher temperature stability and variable gyration resistances. The gyrator may also be made active by choosing $R_a \neq R_b$.

The gyrator is very well suited for the conversion of capacitors to inductors. When loaded at port 1 in a capacitor C_B, an equivalent inductance L_{equiv} $(= R_G^2 C_B)$ is seen at port 2. By measuring the bandwidth $\mathscr{B}$ and resonant frequency ω_0 of the frequency response, when loaded at port 2 in a variable C_A and fed with a current source (1·5MΩ resistor in series with a signal generator), the measured Q $(= \omega_0/\mathscr{B})$ (Reference 18, p. 355) was obtained for Fig. 2A; the maximum Q factor

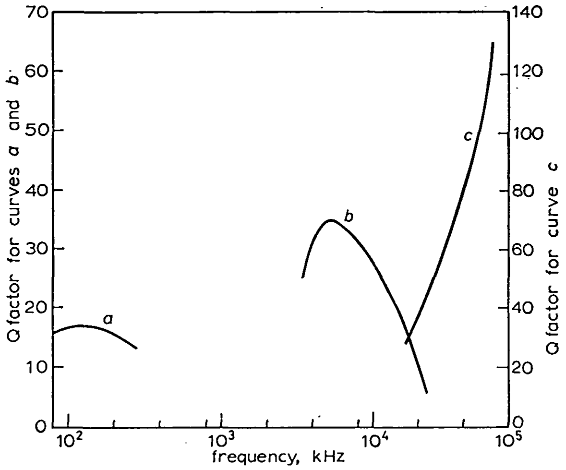

Fig. 2A *Measured Q factor against frequency*
a $C_B = 0{\cdot}47\mu F$; equivalent inductance = 4·9H
b $C_B = 0{\cdot}01\mu F$; equivalent inductance = 0·1H
c $C_B = 1200pF$; equivalent inductance = 0·013H

occurs at $\omega_{max} = 1/R_G C_B = 1/\sqrt{(R_G^2 C_B C_A)}$ (Reference 19, Fig. 3), or at $C_A = C_B$, which was checked experimentally. The circuit was stable at frequencies below 65kHz, with measured equivalent inductances very close to estimated values. When the circuit was lightly loaded, it became oscillatory at frequencies above 65kHz. When shunted with a 100kΩ resistor, the circuit maintained stable operation at 100kHz; as expected, the shunt resistance drastically reduced the effective Q factor. It should be observed that, when one port is loaded with a capacitor, the d.c. offset voltage is less than 100mV. The gyrator behaved identically when the ports were interchanged.

In summary, an integrated direct-coupled gyrator has been described; a photomicrograph is shown in Fig. 2B. Coupled

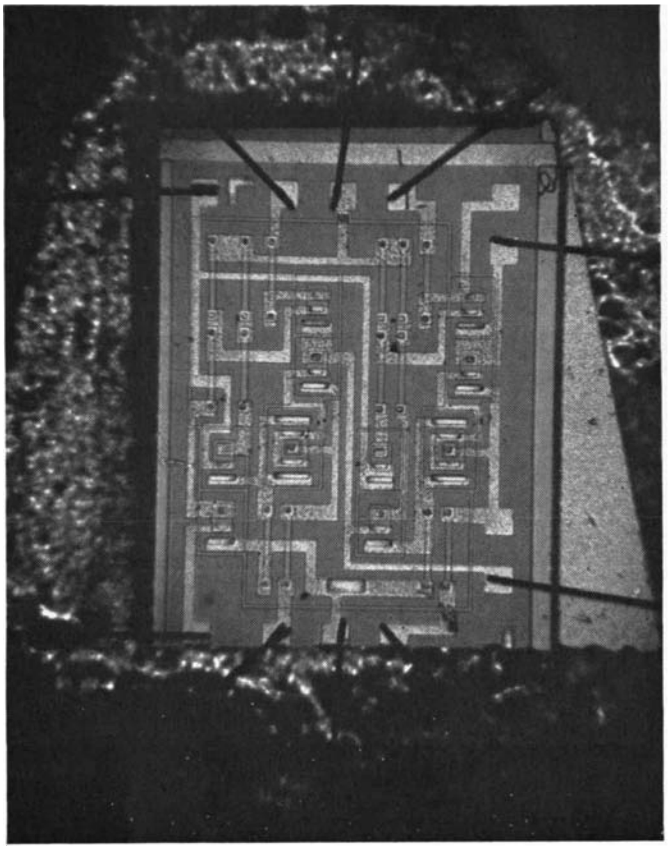

Fig. 2B *Photomicrograph of integrated gyrator*

with recent results on gyrator RC filters,[20,21] this shows the practical possibility of integrated filters and other devices; for example, delay lines,[22] mixers[23] and tunable structures.[24] Further work on such integrated components is continuing, and it is hoped to report on these, on high-frequency behaviour of the gyrator and on the properties of integrated time-variable gyrators in the future.

Table 1 MEASURED PARAMETERS

	Supply voltages, V_0 = 5V					
	Z_{in} port 1		Z_{in} port 2		Open-circuit offset voltage	
	Port 2 open	Port 2 earthed	Port 1 open	Port 1 earthed	Port 1	Port 2
Unit 1	50Ω	208kΩ	40Ω	200kΩ	−60mV	98mV
Unit 2	40Ω	250kΩ	43Ω	200kΩ	−20mV	76mV

	Supply voltages, V_0 = 5V				
	Gyration resistance R_G (design R_G = 3kΩ)			Linear dynamic range	
	25°C	50°C	100°C	Voltage	Current
Unit 1	3·16kΩ	3·24kΩ	3·33kΩ	±2·5V	±0·9mA
Unit 2	3·23kΩ	3·24kΩ	3·37kΩ	±2·4V	±0·85mA

The authors wish to express their sincere appreciation for the technical assistance and consultation of D. Rosprim of Fairchild Semiconductor for the integration of the circuit.

H. T. CHUA
R. W. NEWCOMB

4th April 1967

Stanford Electronics Laboratories
Stanford, Calif. 94305, USA

References

1 SHEAHAN, D. F., and ORCHARD, H. J.: 'Integratable gyrator using m.o.s. and bipolar transistors', *Electronics Letters*, 1966, **2**, 390–391
2 WITT, F. J.: 'Nonreciprocal wave translating network', United States Patent 3109147, 1963
3 SHENOI, B. A.: 'Practical realization of a gyrator circuit and *RC*-gyrator filters', *IEEE Trans.*, 1965, **CT-12**, pp. 374–380
4 NEW, W., and NEWCOMB, R.: 'An integratable time-variable gyrator', *Proc. Inst. Elect. Electronics Engrs.*, 1965, **53**, pp. 2161–2162
5 SHEAHAN, D. F., and ORCHARD, H. J.: 'High-quality transitorised gyrator', *Electronics Letters*, 1966, **2**, pp. 274–275
6 GENSEL, J.: 'Negative Widerstände und Gyratoren', *Nachrichtentechnik*, 1957, **7**, pp. 249–256
7 HARRISON, T. J.: 'A gyrator realization', *IEEE Trans.*, 1963, **CT-10**, p. 303
8 GHAUSI, M. S., and MCCARTHY, F. D.: 'A realization of transistor gyrators', *Semiconductor Prod. Solid State Technol.*, 1964, October, pp. 13–17
9 VASUDEVA, M. S., 'Gyrator realization', *Electronics Letters*, 1966, **2**, pp. 201–202
10 SU, K. L.: 'A transistor-circuit realization of the inductance', *Proc. Inst. Elect. Electronics Engrs.*, 1966, **54**, pp. 2025–2027
11 SHEAHAN, D. F.: 'Gyrator-floatation circuit', *Electronics Letters*, 1967, **3**, pp. 39–40
12 MORSE, A. S., and HEULSMAN, L. P.: 'A gyrator realization using operational amplifiers', *IEEE Trans.*, 1964, **CT-11**, pp. 277–278
13 HOLMES, W. H., GRUETZMANN, S., and HEINLEIN, W. E.: 'High-performance direct-coupled gyrators', *Electronics Letters*, 1967, **3**, pp. 45–46
14 HOLMES, W. H., GRUETZMANN, S., and HEINLEIN, W. E.: 'Direct-coupled gyrators with floating ports', *ibid.*, 1967, **3**, pp. 46–47
15 BUTLER, F.: 'Gyrators using direct-coupled transistor circuits', *Wireless World*, 1967, **73**, pp. 89–93
16 RAO, T. N., and NEWCOMB, R. W.: 'Direct-coupled gyrator suitable for integrated circuits and time variation', *Electronics Letters*, 1966, **2**, pp. 250–251
17 LIN, H. C., TAN, T. B., CHANG, G. Y., VAN DER LEEST, B., and FORMIGONI, N.: 'Lateral complementary transistor structure for the simultaneous fabrication of functional blocks', *Proc. Inst. Elect. Electronics Engrs.*, 1966, **52**, pp. 1491–1495
18 VAN VALKENBURG, M. E.: 'Network analysis', (Prentice-Hall, NJ, 1964), 2nd edn.
19 RAO, T. N., GARY, P., and NEWCOMB, R. W.: 'Equivalent inductance and *Q* of a capacitor loaded gyrator', *IEEE J. Solid-State Circuits*, to be published
20 SHEAHAN, D. F., and ORCHARD, H. J.: 'Bandpass-filter realization using gyrators', *Electronics Letters*, 1967, **3**, pp. 40–42
21 NEWCOMB, R. W., RAO, T. N., and WOODARD, J.: 'A minimal capacitor cascade synthesis for integrated circuits', *Microelectronics and and Reliability*, to be published
22 ANDERSON, B. D., BRADY, D. M., NEW, W., and NEWCOMB, R.: 'A tapped electronically variable delay line suitable for integrated circuits', *Proc. Inst. Elect. Electronics Engrs.*, 1966, **54**, pp. 1118–1119
23 ANDERSON, B. D., NEW, W., and NEWCOMB, R. W.: 'Oscillators, modulators and mixers suitable for integrated circuit realization', *ibid.*, to be published
24 ANDERSON, B. D., NEW, W., and NEWCOMB, R. W.: 'Proposed adjustable tuned circuits for microelectronic structures', *ibid.*, 1966, **54**, p. 411

ASYMPTOTIC SOLUTION OF OBLIQUE WAVES IN INHOMOGENEOUS VERTICALLY MAGNETISED PLASMA*

A method for finding higher-order asymptotic solutions, as compared with the well known WKBJ approximation, is given for oblique electromagnetic waves in an inhomogeneous anisotropic plasma with a vertical magnetostatic field.

One of the most important methods of solving the problem of oblique incidence of waves on a layer of magnetoplasma are the WKBJ solutions, which have been used by Clemmow and Heading[1] and Budden and Clemmow[2] for the solution of first-order coupled equations by a successive-approximation method. The WKBJ solution is usually recognised as a first approximation of an asymptotic solution. However, the procedure of finding higher-order asymptotic solutions is found to be either inadequate or rather involved. Recently, a simpler procedure of finding higher-order solutions as correction terms to the WKBJ solution has been suggested[3,4] for the case of an isotropic layer of plasma. The aim of the present letter is to apply this procedure to the solution of the fourth-order differential equations governing the oblique propagation of waves in an inhomogeneous plasma with imposed vertical static magnetic field.

Starting from Maxwell's equations one could obtain[5] the general wave equation for a plasma medium:

$$\nabla^2 E_i - \frac{\partial}{\partial x_i}(\nabla . E) + k^2 \epsilon_{il}(z, k)E_l = 0 \quad . \quad . \quad . \quad (1)$$

where one defines

$k = \omega\sqrt{(\mu\epsilon)} = \omega/c$ = free-space wave number

$\epsilon_{il}(z, k)$ = complex permittivity tensor

Eqn. 1 has a solution of the type

$$E(r) = F(z)\, e^{-ikpy} \quad . \quad . \quad . \quad . \quad . \quad . \quad . \quad . \quad . \quad (2)$$

corresponding to waves with normals in the yz plane, where $p = \sin\theta_I$ and $\partial/\partial x \equiv 0$. Assuming the static magnetic field $H_0(z)$ in the z direction, and substituting eqn. 2 into eqn. 1, one obtains two second-order coupled equations after eliminating F_z:

$$\frac{d^2F_x}{dz^2} + k^2(\epsilon_{xx} - p^2)F_x + k^2\epsilon_{xy}F_y = 0 \quad . \quad . \quad . \quad (3a)$$

$$(1 + p^2A_0)\frac{d^2F_y}{dz^2} + p^2\frac{dA_0}{dz}\frac{dF_y}{dz} + k^2\epsilon_{yy}F_y + k^2\epsilon_{yx}F_x = 0 \quad . \quad (3b)$$

where one defines:[5,6]

$$A_0(z) = \frac{1}{\epsilon_{zz} - p^2}$$

$$\epsilon_{xx}(z, k) = 1 - \frac{XU}{U^2 - Y^2}$$

$$\epsilon_{yy}(z, k) = 1 - \frac{XU^2}{U(U^2 - Y^2)}$$

$$\epsilon_{zz}(z, k) = 1 - \frac{X}{U}$$

$$\epsilon_{xy}(z, k) = -\epsilon_{yx}(z, k) = \frac{-iXY}{U^2 - Y^2}$$

and $Y = Y_z = \dfrac{\omega_{Hz}}{k};\ X = \dfrac{e^2N(z)}{m\epsilon_0\omega^2} = \dfrac{aN(z)}{k^2};\ U = 1 - iZ$

$$a = \frac{e^2}{\epsilon_0 mc^2};\ \omega_{Hz} = \frac{e\mu_0}{mc}H_0$$

Eqns. 3 could be combined give a fourth-order differential equation for F_y and F_x as follows[7]:

$$F^{\rm IV} + \alpha(z,k)F^{\rm III} + \beta(z,k)F^{\rm II} + \gamma(z,k)F^{\rm I} + \delta(z,k)F = 0 \quad . \quad (4)$$

where $F = F_x$ or $F = F_y$, and one has[7]

$$\alpha(z,k) = \alpha_0(z) + \frac{i}{k}\alpha_{-1}(z) + \frac{\alpha_{-2}}{k^2} + \ldots$$

$$\beta(z,k) = \beta_2(z)k^2 + \beta_1(z)ik + \beta_0(z) + \ldots$$

$$\gamma(z,k) = \gamma_2(z)k^2 + \gamma_1(z)ik + \gamma_0(z) + \frac{\gamma_{-2}}{k^2} + \ldots$$

$$\delta(z,k) = \delta_4(z)k^4 + \delta_2k^2 + \delta_1(z)ik + \delta_0(z) + \ldots$$

Asymptotic solutions will be found below for F_y only using eqn. 4, and the procedure can be repeated to solve for F_x.

Assuming a solution in the form

$$F_y(z) = \exp\left\{ik\int^z \phi(z,k)dz\right\} \quad . \quad . \quad . \quad . \quad . \quad . \quad (5a)$$

* The research reported here was supported in part by the US National Science Foundation